

引用格式：刘奎，陈宣华，王德润，等，2024. 北山东南部早白垩世伸展构造变形：二维反射地震剖面解释与磷灰石裂变径迹测年的制约[J]. 地质力学学报, 30 (3) : 377–393. DOI: [10.12090/j.issn.1006-6616.2023151](https://doi.org/10.12090/j.issn.1006-6616.2023151)

Citation: LIU K, CHEN X H, WANG D R, et al., 2024. The Early Cretaceous extensional deformation in the southeastern Beishan Range, central Asia: Constrains from 2D seismic reflection profile interpretation and apatite fission track thermochronology[J]. Journal of Geomechanics, 30 (3) : 377–393. DOI: [10.12090/j.issn.1006-6616.2023151](https://doi.org/10.12090/j.issn.1006-6616.2023151)

## 北山东南部早白垩世伸展构造变形：二维反射地震剖面解释与磷灰石裂变径迹测年的制约

刘 奎<sup>1</sup>, 陈宣华<sup>1</sup>, 王德润<sup>2</sup>, 顾文沛<sup>2</sup>, 邵兆刚<sup>1</sup>, 张义平<sup>1</sup>  
LIU Kui<sup>1</sup>, CHEN Xuanhua<sup>1</sup>, WANG Derun<sup>2</sup>, GU Wenpei<sup>2</sup>, SHAO Zhaogang<sup>1</sup>, ZHANG Yiping<sup>1</sup>

1. 中国地质科学院地球深部探测中心, 北京 100037;
  2. 中国石油集团东方地球物理勘探有限责任公司吐哈物探处, 新疆 哈密 839000
1. *SinoProbe Center, Chinese Academy of Geological Sciences, Beijing 100037, China;*  
2. *Tuha Division, Bureau of Geophysical Prospecting INC., China National Petroleum Corporation, Hami 839000, Xinjiang, China*

### The Early Cretaceous extensional deformation in the southeastern Beishan Range, central Asia: Constrains from 2D seismic reflection profile interpretation and apatite fission track thermochronology

**Abstract:** [Objective] The Beishan Range occupies a key position in Central Asia. This study aims to deepen the understanding of the timing, intracontinental deformation processes, and their dynamic mechanisms in the Late Mesozoic on the southern margin of the Central Asian Orogenic Belt (CAOB). [Methods] We conducted detailed analyses of the Early Cretaceous extensional and earlier compressional structures in the southeastern Beishan Range through field geological observations, interpretation of 2D reflection seismic profiles, and apatite fission track thermochronology. [Conclusion] Field observations show that Lower–Middle Jurassic strata have been strongly deformed by numerous thrusts and folds. 2D seismic reflection profiles reveal two NE- to NEE-striking normal faults. The Suosuojing fault is a SE-dipping low-angle listric normal fault, while the Wudaoming fault is a NW-dipping high-angle normal fault. These normal faults cut through the early-formed fold-thrust system, indicating a transition from contraction to extension. The Suosuojing and Wudaoming faults, respectively, define the northwestern and southeastern boundaries of the Early Cretaceous Zongkouzi basin. The Zongkouzi basin exhibits a graben geometry, with Lower Cretaceous strata displaying typical growth-strata relationships, suggesting that the normal faults were active during the late Early Cretaceous. Thermal history modeling results from apatite fission track data indicate that the footwall of the Suosuojing fault experienced rapid cooling between 132 and 110 Ma. This rapid cooling phase was closely related to the footwall exhumation during the normal slip of the Suosuojing fault. We argue that the Late Mesozoic intracontinental contraction–extension transition in the southeastern Beishan Range likely occurred between ~133 Ma and ~129 Ma in the late Early Cretaceous. The collapse of the thickened crust and coupled mantle upwelling triggered the Early Cretaceous extensional deformation in the southern CAOB.

基金项目：中国地质调查局地质调查项目（DD20230229, DD20221643, DD20190011, DD20160083）

This research is financially supported by the Geological Survey Project of the China Geological Survey (Grants No. DD20230229, DD20221643, DD20190011, and DD20160083).

第一作者：刘奎（1991—），男，在读博士，主要从事构造变形与构造–热年代学的研究工作。Email: [kuiliucags@foxmail.com](mailto:kuiliucags@foxmail.com)

通讯作者：陈宣华（1967—），男，研究员，主要从事大地构造与构造地质学、地球深部探测与深地科学等研究工作。

Email: [xhchen@cags.ac.cn](mailto:xhchen@cags.ac.cn)

收稿日期：2023-09-11；修回日期：2023-12-04；录用日期：2023-12-05；网络出版日期：2023-12-05；责任编辑：范二平

**Keywords:** Beishan; Early Cretaceous; extensional tectonic deformation; apatite fission track; contraction–extension transition

**摘要:** 为深入认识中亚造山带南缘晚中生代陆内变形过程及其动力学机制,通过野外地质观察、二维反射地震剖面解释及磷灰石裂变径迹测年,对北山东南部早白垩世伸展构造及早期挤压构造进行了详细解析。结果表明,一系列逆冲断层与褶皱构造造成下—中侏罗统发生强烈的挤压变形。地震剖面揭示出2条早白垩世伸展正断层,其中梭梭井断层为南东倾向的低角度铲式正断层,五道明断层为北西倾向的高角度正断层,二者共同切割了早期形成的褶皱-冲断系统,指示挤压-伸展构造的转换;梭梭井断层与五道明断层分别限定了早白垩世总口子盆地的北西和南东边界,使得其具有“地堑”样式,盆地内沉积的下白垩统生长地层发育,表明伸展正断层的活动时间为早白垩世晚期。磷灰石裂变径迹热史模拟结果显示,梭梭井断层下盘于132~110 Ma经历了快速冷却和剥露事件,该事件与其持续的正断层活动密切相关,进一步证实北山东南部晚中生代挤压-伸展构造的转换很可能发生在早白垩世晚期(133~129 Ma)。增厚地壳的重力垮塌与局部地幔上涌共同导致了中亚造山带南缘早白垩世的区域伸展作用。

**关键词:** 北山;早白垩世;伸展构造变形;磷灰石裂变径迹;挤压-伸展构造转换

中图分类号: P542; P548 文献标识码: A 文章编号: 1006-6616 (2024) 03-0377-17

DOI: 10.12090/j.issn.1006-6616.2023151

## 0 引言

中亚地区发育众多典型的陆内变形的实例,如新生代的天山、阿勒泰及祁连山等(Yin et al., 1998; Cunningham, 2005; Jolivet et al., 2010; Zuza et al., 2018)。在新生代印度-亚洲板块碰撞之前,中亚地区中生代经历了极其复杂的变形过程(Zheng et al., 1996; Dumitru and Hendrix, 2001; Jolivet et al., 2001; Darby and Ritts, 2002; Wang et al., 2022),记录了亚洲陆缘不同块体之间多期汇聚与碰撞拼贴的过程(Darby and Ritts, 2002; Dong et al., 2015; 董树文等, 2019; Chen et al., 2022; Liu et al., 2023)。另外,中生代复杂的变形模式很有可能影响到了中亚地区新生代的构造变形分布(Dumitru et al., 2001; Jolivet et al., 2001, 2010; Zuza et al., 2018; Cheng et al., 2019)。因此,中亚地区成为研究陆内变形过程和探讨变形机制的热点地区(Cunningham, 2005; Raimondo et al., 2014)。

北山位于中亚造山带的最南缘,同时紧邻特提斯-喜马拉雅-青藏高原造山带的最北缘,构造位置十分关键(Wang et al., 2010; Xiao et al., 2010; Li et al., 2023)。已有研究表明,晚中生代陆内挤压变形将古生代—早中生代北山造山带构造活化,形成了北山褶皱-冲断带(左国朝等, 1992; Zheng et al., 1996; Dumitru and Hendrix, 2001; Liu et al., 2023)。北山褶

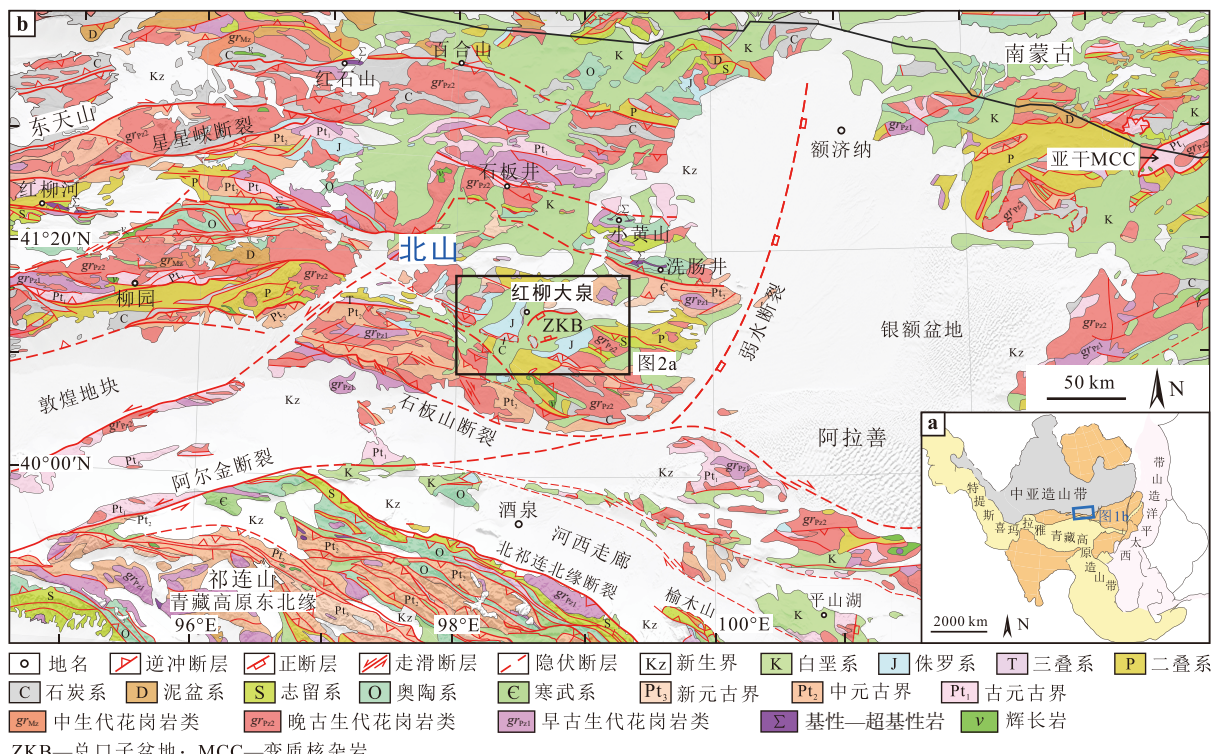
皱-冲断带开始形成于中侏罗世晚期,挤压逆冲作用可能一直持续到早白垩世。同时,热年代学数据也记录了早白垩世晚期(124~115 Ma)与正断层活动相关的下盘剥露与冷却事件,指示晚中生代北山褶皱-冲断带经历了挤压-伸展构造的转换(Liu et al., 2023)。区域上,这一构造转换普遍存在于中亚造山带南缘,形成了众多叠加于褶皱-冲断带或增厚地壳之上的正断层、断陷盆地及变质核杂岩等(Webb et al., 1999; Johnson et al., 2001; Chen et al., 2003; Meng, 2003; Cunningham et al., 2009; Wang et al., 2011; 朱日祥等, 2012; Lin et al., 2013; Zhu et al., 2015)。截至目前,部分学者认为北山、南蒙古及阿拉善地区伸展构造变形开始于晚侏罗世(Zheng et al., 1996; Graham et al., 2001; Meng, 2003)。然而,诸多研究成果表明区域伸展作用开始于早白垩世(Davis et al., 2002; Davis and Darby, 2010; 张长厚等, 2011; Wang et al., 2018; Lin et al., 2019, 2020; Liu et al., 2023)。同时,相关学者提出了多种关于中亚造山带南缘晚中生代陆内伸展构造变形的动力学模式,包括增厚地壳的重力垮塌(Meng, 2003; Wang et al., 2011)、古太平洋板块俯冲后撤引发的弧后伸展(朱日祥等, 2011, 2012; Zuo et al., 2020; Hui et al., 2021)及岩浆底侵(张宇等, 2024)等。但是,在北山地区仍缺少针对该期伸展构造变形样式、模式及起始时间等的研究。这些争议和不足制约了对中亚造山带南缘晚中生代陆内变形过程及其动力学机

制的认识。

为解决上述问题, 文章选择北山东南部红柳大泉地区作为研究区。基于卫星影像解译与野外地质观察, 分析了下—中侏罗统和下白垩统的构造变形特征; 并通过开展二维反射地震剖面解释, 详细解析了研究区内的伸展构造变形特征; 此外, 根据磷灰石裂变径迹测年及热史模拟结果, 进一步限定了伸展构造变形的时间。这些研究对深入认识中亚造山带南缘晚中生代陆内挤压—伸展构造转换及其动力学模式具有重要作用。

## 1 区域地质背景

北山位于中亚造山带的最南缘(图1a; Zuo et al., 1991; Xiao et al., 2010; Li et al., 2023; 唐卫东等, 2023), 呈近东西向展布, 北接南蒙古构造带, 往西以星星峡断裂为界与东天山相接, 南邻敦煌地块与河西走廊, 往东与阿拉善地块相接(图1b; Zuo et al., 1991; Wang et al., 2010; Xiao et al., 2010; Feng et al., 2018; Zhang et al., 2021a, 2022; 贺昕宇等, 2022)。



a—亚洲大地构造简图; b—北山地区及周缘区域地质图

图1 亚洲大地构造简图与北山地区及其周缘区域地质图(任纪舜等, 2013; 徐学义等, 2015; 陈宣华等, 2019; Liu et al., 2023)

Fig. 1 Sketched tectonic map of Asia and regional geologic map of the Beishan Range and its surrounding belts, central Asia(modified from Ren et al., 2013; Xu et al., 2015, Chen et al., 2019; Liu et al., 2023)

(a) Sketched tectonic map of Asia; (b) Regional geologic map of the Beishan Range and its surrounding belts

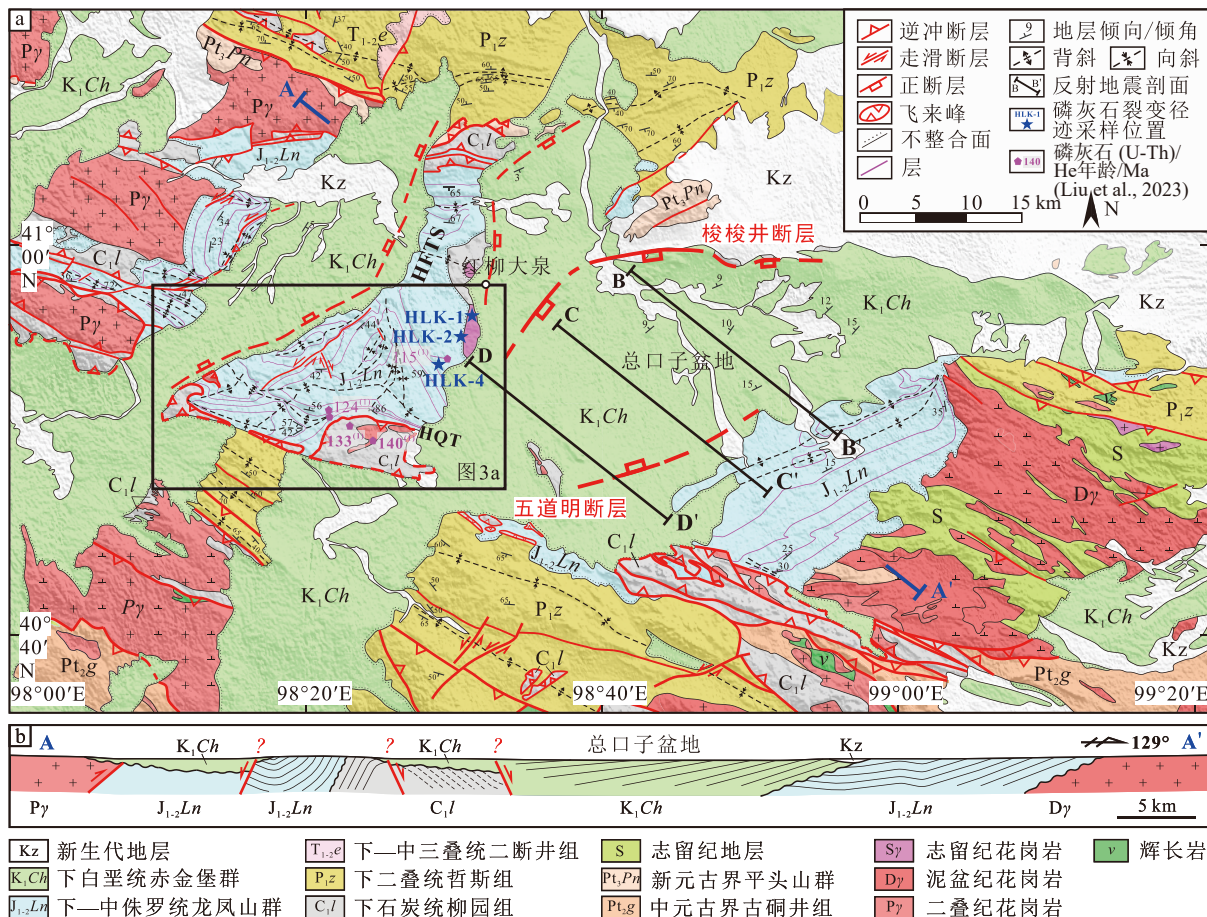
ZKB—Zongkouzi Basin; MCC—metamorphic core complex

北山地区出露前寒武纪地层, 古生代与俯冲、裂谷及碰撞造山作用相关的岩浆岩和变质岩, 古生代海相沉积地层, 以及中—新生代陆相沉积地层(甘肃省地质局和第二区域地质调查队, 1971; Xiao et al., 2010; Song et al., 2013; Cleven et al., 2018; He et al., 2018; Li et al., 2023)。北山东南部下石炭统柳园

组( $C_1l$ )主要由流纹斑岩、安山岩、凝灰质砂岩、砂岩和灰岩组成(甘肃省地质局和第二区域地质调查队, 1971; 靳拥拥护等, 2020); 下二叠统哲斯组( $P_1z$ )岩性为玄武岩、安山岩、凝灰岩、砾岩、砂岩及灰岩等(甘肃省地质局和第二区域地质调查队, 1971); 下—中侏罗统龙凤山群( $J_{1-2}L_n$ )由底部厚层砾岩和中—

上部的含砾粗砂岩、砂岩、粉砂岩及粉砂质泥岩组成(甘肃省地质局和第二区域地质调查队, 1971; 牛海青等, 2021); 下白垩统赤金堡群( $K_1Ch$ )分布极为广泛(图 1b, 图 2a), 主要由砾岩、砂岩、泥质粉砂岩

和页岩组成(Li et al., 2007; 彭楠等, 2013; 张金龙等, 2017; 任文秀等, 2022)。新生代地层厚度很薄, 为一套冲积扇与河流相沉积(甘肃省地质局和第二区域地质调查队, 1971)。



a—红柳大泉地区地质图; b—北西—南东走向 AA'剖面图

图 2 北山东南部红柳大泉地区地质图(底图据甘肃省地质局和第二区域地质调查队, 1971; 斯拥护等, 2020 修改)

Fig. 2 Geologic map of the Hongliudaquan area, southeastern Beishan Range (base map modified from BGGP, 1971; Jin et al., 2020; Apatite (U-Th)/He ages according to Liu et al., 2023)

(a) Geological map of the Hongliudaquan area; (b) NW–SE trending section AA'

HFTS—Hongliudaquan Fold-Thrust System; HQT—Hongqishan Thrust Fault

北山造山带形成于古生代—早中生代时期古亚洲洋多个分支洋盆长期俯冲消减、增生及最终闭合的过程中(Xiao et al., 2010; Ao et al., 2012; Song et al., 2013; He et al., 2018; Li et al., 2023)。随后, 强烈的陆内挤压变形将其构造活化, 形成了晚中生代北山褶皱–冲断带。其中, 北山逆冲推覆构造将大量中元古界白云质灰岩和大理岩等往北逆冲推覆至新元古界至下一中侏罗统之上, 其推覆距离至少约

为 120 km(左国朝等, 1992; Zheng et al., 1996)。在北山东南部, 红柳大泉褶皱–冲断系统将下—中侏罗统强烈挤压变形(图 2a; Liu et al., 2023)。该挤压变形系统沿南北和北西—南东 2 个方向同时发生水平缩短(收缩变形)。红柳大泉褶皱–冲断系统被下白垩统不整合覆盖(图 2)。区域上, 早白垩世地层普遍被认为沉积在一系列地堑/半地堑盆地中(Meng, 2003; Meng et al., 2003; 张金龙等, 2017; Hui et al.,

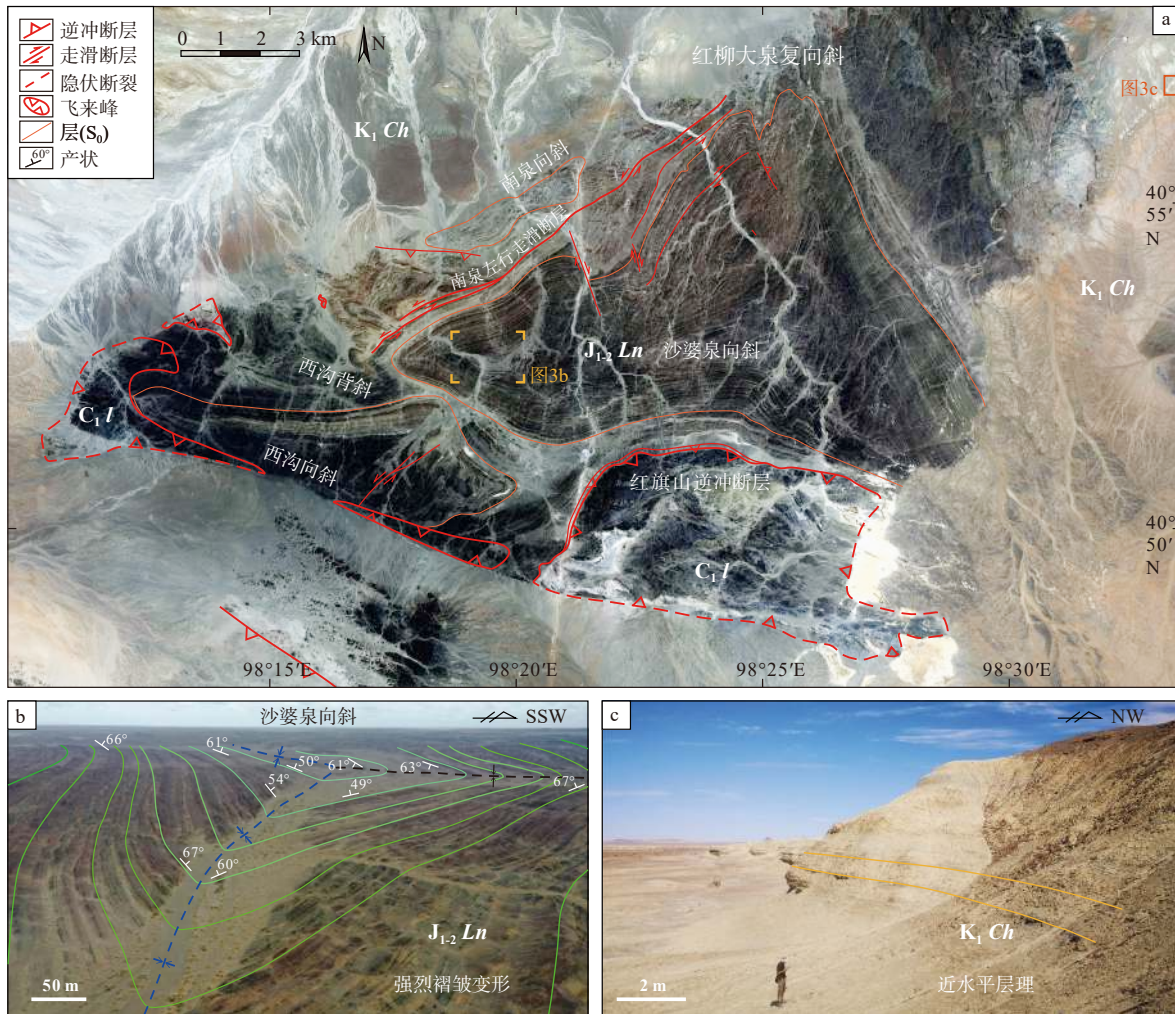
2021), 或部分逆冲断层被晚期的正断层或大型拆离断层所切割, 指示区域性的伸展构造变形(Zheng et al., 1996; Webb et al., 1999; Graham et al., 2001; Meng, 2003; Meng et al., 2003)。北山地区新生代的构造活动很弱(陈柏林等, 2003; Cunningham, 2013; 云龙等, 2021)。

## 2 构造变形分析

### 2.1 卫星影像解译与野外地质观察

在北山东南部红柳大泉地区, 下一中侏罗统龙凤山群( $J_{1-2}Ln$ )广泛分布(图2a)。其南侧北西—

南东东走向的红旗山逆冲断层将下石炭统柳园组及早二叠世花岗岩体往北逆冲推覆至下一中侏罗统之上(图2a, 图3a)。同时, 一系列千米级别的构造盆地和短轴背斜/穹隆构造造成下一中侏罗统发生强烈褶皱变形, 如红柳大泉复向斜(图3a, 图3b), 其形状呈不规则的三角形、拉长的椭圆形及变形虫等, 其枢纽沿多个方向展布, 包括北北西向、东西向、北西向和北南向(图2a, 图3a)。此外, 褶皱系统内部还发育一些次级的走滑断层(图3a)。这些逆冲断层、褶皱及走滑断层等共同组成了红柳大泉褶皱-冲断系统(Liu et al., 2023)。上述结果表明, 北山东南部晚中生代经历了强烈的挤压构造变形。



a—谷歌地球卫星影像的构造解译图; b—发育于下一中侏罗统内部的挤压构造变形的野外照片; c—下白垩统的野外照片

图3 北山东南部红柳大泉地区构造解译图与野外照片 (Liu et al., 2023)

Fig. 3 Google Earth satellite image and field photos showing the structural deformation of the  $J_{1-2}Ln$  and  $K_1Ch$  groups in the Hongliudaquan area, southeastern Beishan Range (Liu et al., 2023)

(a) Google Earth satellite image showing the structural deformation; (b) Field photo of the  $J_{1-2}Ln$  group; (c) Field photo of the  $K_1Ch$  group

下白垩统赤金堡群( $K_1Ch$ )大面积出露于北山东南部(图2a, 图3a)。相较于强烈挤压变形的下一中侏罗统(图3b),早白垩世地层的变形程度很弱(图3c)。同时,研究区地形起伏低且地表覆盖较严重,很难通过野外地质观察揭示早白垩世总子盆地的构造样式及属性等信息。

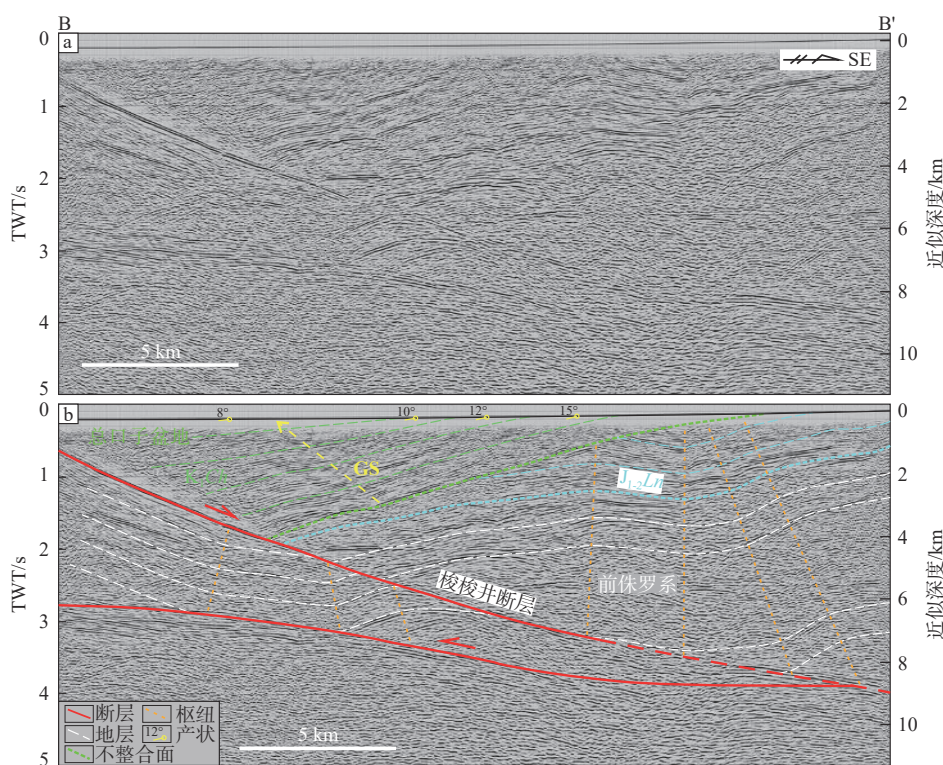
## 2.2 二维反射地震剖面解释

为解决上述问题,在北山东南部红柳大泉地区选取了3条北西—南东走向的二维反射地震剖面。在对地震剖面进行解释时,首先将地震剖面由时间域剖面转为深度域剖面。随后,按照地震剖面构造解释的基本步骤开展解释工作,具体步骤见陈宣华等(2010)。基于上述工作,在北山东南部识别出了2条早白垩世伸展正断层,即梭梭井断层与五道明断层(图2a)。

### 2.2.1 正断层与断陷盆地

在地震剖面BB'上,梭梭井断层的地震反射特征为一个强反射界面,其延续性很好,从双程走时

(TWT)~0.6 s往下延续至~3.7 s(图4a)。在强反射界面之上,下白垩统赤金堡群( $K_1Ch$ )表现为弱一中等振幅、连续性较好、平行反射,其同相轴与强反射界面呈大角度的斜交关系(图4b)。下一中侏罗统龙凤山群( $J_{1-2}Ln$ )的反射特征以中等振幅、中等连续、亚平行为主。同时,下白垩统与下一中侏罗统之间发育一个角度不整合面(图4b)。在强反射界面之下,前侏罗系的反射特征以中等振幅-杂乱反射为主,其同相轴的连续性一般(图4b)。在地震剖面BB'和CC'上,梭梭井断层的地震反射特征类似(图4, 图5)。在地震剖面DD'上没有发育类似梭梭井断层的强反射界面(图6a),在剖面西段下白垩统不整合于下一中侏罗统及前侏罗系之上(图2a, 图6b)。该不整合面从近地表(~0 s)往下延伸至~1.5 s(图6b);剖面东段发育一个较弱的断层反射界面(图6a),其与下白垩统反射同相轴呈大角度的斜交关系,该断层反射界面为五道明断层(图6b)。



a—未解释地震剖面BB'; b—BB'地震剖面的构造解释图

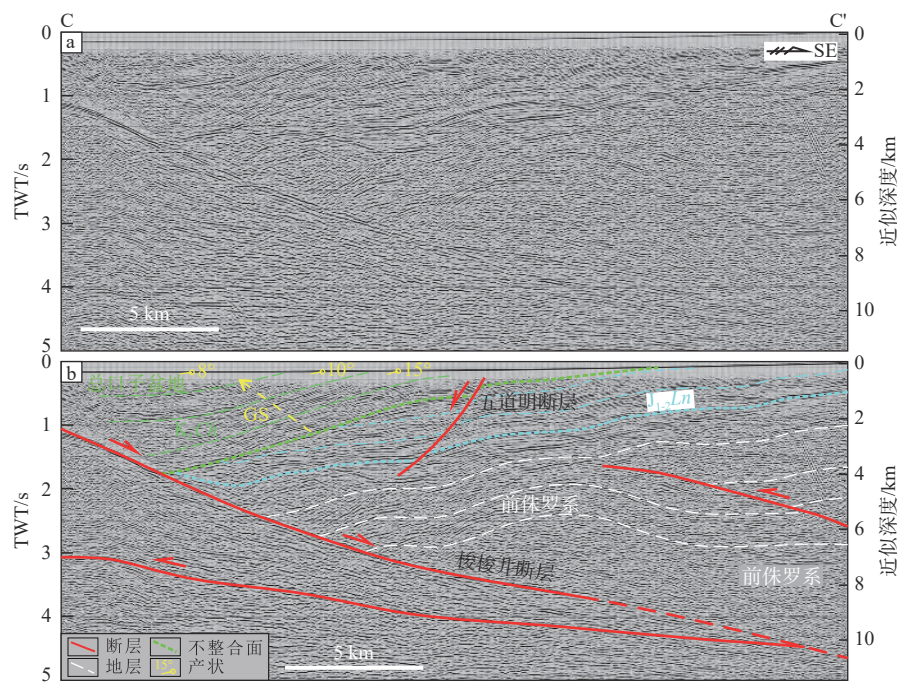
图4 地震剖面BB'及其构造解释特征(剖面位置见图2)

Fig. 4 Seismic profile BB' and its structural interpretation (Profile location is shown in Fig. 2)

(a) Uninterpreted seismic profile BB'; (b) Structural interpretation map of seismic profile BB'

在地震剖面BB'和CC'上,梭梭井断层倾向南东,视倾角从剖面浅部至深部由 $30^\circ\sim24^\circ$ 逐渐变为

$15^\circ\sim10^\circ$ ,并且其往下延伸至8~10 km(图4b, 图5b)。梭梭井断层上盘由 $K_1Ch$ 、 $J_{1-2}Ln$ 及前侏罗系组成,下

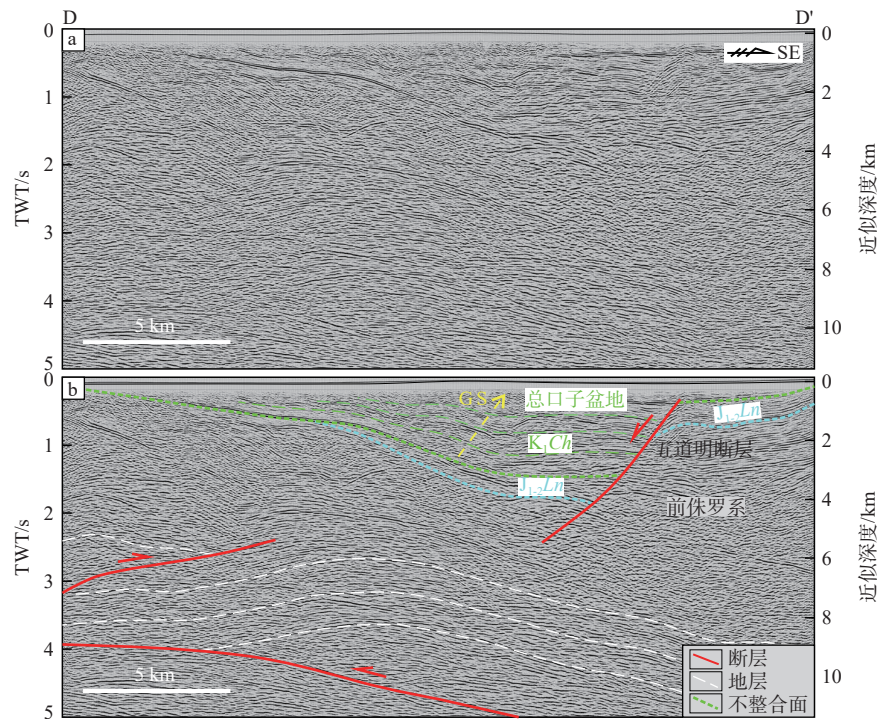


a—未解释地震剖面CC'; b—CC'地震剖面的构造解释图

图5 地震剖面CC'及其构造解释特征(剖面位置见图2)

Fig. 5 Seismic profile CC' and its structural interpretation (Profile location is shown in Fig. 2)

(a) Uninterpreted seismic profile CC'; (b) Structural interpretation map of seismic profile CC'



a—未解释地震剖面DD'; b—DD'地震剖面的构造解释图

图6 地震剖面DD'及其构造解释特征(剖面位置见图2)

Fig. 6 Seismic profile DD' and its structural interpretation (Profile location is shown in Fig. 2)

(a) Uninterpreted seismic profile DD'; (b) Structural interpretation map of seismic profile DD'

盘以前侏罗纪地层为主(图 4b, 图 5b)。在地震剖面 CC'和 DD'上, 五道明断层倾向北西, 倾角明显变陡, 其往下延伸至 5~6 km。五道明断层上盘以下白垩统为主, 下盘为下一中侏罗统与前侏罗系(图 6b)。因此, 梭梭井断层为一条低角度的铲式正断层(图 4b), 五道明断层为一条高角度正断层(图 6b)。平面上, 梭梭井断层的走向为北东—北东东向, 其长度超过 30 km(图 2a)。五道明断层的走向为北东向, 其长度为 10~15 km(图 2a)。

梭梭井断层和五道明断层分别限定了早白垩世总口子盆地的北西和南东边界(图 2a), 二者共同控制了早白垩世总口子盆地的形成和演化。总口子盆地在地震剖面 BB'和 DD'上表现为“半地堑”样式(图 4b, 图 6b), 而在 CC'剖面表现为“地堑”样式(图 5b)。该断陷盆地内  $K_1Ch$  最大沉积厚度为 3~4 km(图 4b, 图 6b)。

## 2.2.2 生长地层

在地震剖面 BB'和 CC'上, 下白垩统赤金堡群( $K_1Ch$ )的地震反射同相轴具有从深部至浅部逐渐变缓的特征, 形成了典型的沉积三角楔(图 4b, 图 5b)。梭梭井断层上盘的下白垩统地层倾角从底部往上逐渐由~15°变为~12°, 并继续往上变为~8°(图 2a, 图 4b; 甘肃省地质局和第二区域地质调查队, 1971)。五道明断层上盘  $K_1Ch$  的地震反射同相轴也呈三角楔形状, 表现为在靠近正断层位置  $K_1Ch$  的厚度最大, 而远离正断层的沉积地层厚度逐渐减薄(图 6b)。上述地震反射特征表明总口子盆地内下白垩统赤金堡群( $K_1Ch$ )发育生长地层, 并且其形成受到梭梭井断层和五道明断层持续正断层活动的控制。因此, 梭梭井断层和五道明断层均为同沉积正断层,  $K_1Ch$  的沉积时代即为正断层的活动时间。

通过分析北山东南部俞井子盆地和公婆泉盆地内的恐龙化石特征, Li et al.(2007)和张茜楠等(2015)将  $K_1Ch$  的沉积时代定为早白垩世 Aptian-Albian 期(122~100 Ma)。根据孢粉组合特征, 任文秀等(2022)将总口子盆地和公婆泉盆地  $K_1Ch$  的沉积时代限定在早白垩世 Hauterivian-Aptian 期(132.6~113 Ma)。此外, 在该套地层中还发现了大量双壳类、腹足类、介形类及植物类等生物化石, 其时代均为早白垩世晚期(即 Hauterivian 期以来; 杨兵等, 2020)。因此, 北山东南部下白垩统赤金堡群( $K_1Ch$ )的沉积时代很可能为早白垩世晚期。

## 2.2.3 挤压构造变形

在地震剖面 BB'上, 梭梭井断层下盘发育一条早期形成的逆冲断层。该逆冲断层从 9~10 km 往上延伸至<6 km, 并且具有断坪-断坡-断坪结构(图 4b); 该逆冲断层上盘还发育一组不对称的背斜-向斜-背斜组合。在梭梭井断层上盘  $J_{1,2}Ln$  已经发生褶皱变形, 形成一组背斜-向斜-背斜组合(图 4b)。在伸展变形之前, 这 2 套背斜-向斜-背斜组合很可能属于同一个褶皱系统, 在后期伸展变形过程中, 梭梭井断层将其错断。在地震剖面 CC'与 DD'上, 梭梭井断层与五道明断层也均切割了早期形成的挤压构造变形(图 5b, 图 6b)。

## 3 磷灰石裂变径迹测年

### 3.1 样品与实验方法

为更好地揭示北山东南部晚中生代断裂系统的发育过程和构造-热演化历史, 在梭梭井断层下盘采集了 3 块岩石样品, 用于开展磷灰石裂变径迹测试。其中, 样品 HLK-1 采集自志留纪花岗岩体, 采样位置靠近梭梭井断层; 其余 2 块样品(HLK-2、HLK-4)分别为  $J_{1,2}Ln$  花岗岩砾石和含砾粗砂岩, 采样位置逐渐远离梭梭井断层(图 2a)。

3 块样品的磷灰石裂变径迹测试工作在中国地震局地质研究所实验测试中心裂变径迹实验室完成。实验首先将筛选、分离、提纯的磷灰石颗粒用环氧树脂固定在光片上, 进行研磨和抛光处理, 使矿物颗粒内表面露出。随后, 在 21℃ 恒温条件下, 用 5.5% 的  $HNO_3$  蚀刻磷灰石 20 s, 揭示出自发裂变径迹。实验采用外探测器法确定磷灰石裂变径迹年龄。将光片紧贴在低 U 白云母外探测片上, 并连同美国国家标准 CN5 标准玻璃一起放入美国俄勒冈 $^{235}U$  中子活化反应堆进行辐照。照射完成后, 将白云母外探测器片在室温条件下用 40% HF 蚀刻 40 min 后, 揭示出白云母诱发径迹。径迹统计使用 Zeiss Axioplan 2 显微镜, 在放大 1000 倍干镜条件下完成。年龄计算采用 IUGS 推荐的 Zeta 标定方法(Hurford and Green, 1983), 所用 Zeta 常数为  $353.0 \pm 20$ 。年龄校正采用 Durango 磷灰石( $31.4 \pm 0.5$  Ma)作为标准。

### 3.2 测试结果

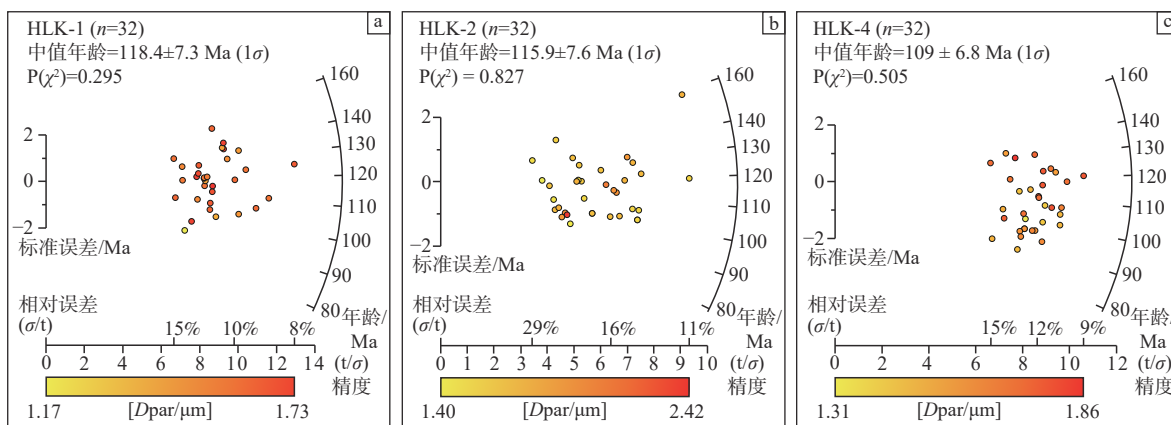
测试结果显示, 3 块样品的磷灰石裂变径迹中值年龄范围为  $118.4 \pm 7.3 \sim 109 \pm 6.8$  Ma(表 1, 图 7), 均处在早白垩世晚期, 并且均小于采样层位的岩体侵

表1 北山东南部红柳大泉地区磷灰石裂变径迹测试结果

Table 1 Apatite fission track results in the Hongliudaquan area, southeastern Beishan Range

样品编号	采样位置/ 高程	$N_c$	$\rho_d \times 10^6$ $\text{cm}^{-2}(N_d)$	$\rho_s \times 10^6$ $\text{cm}^{-2}(N_s)$	$\rho_i \times 10^6$ $\text{cm}^{-2}(N_i)$	$U/\times 10^6$	$P(\chi^2)/\%$	平均径迹长度/ ( $\mu\text{m} \pm 1\text{SD}$ )( $N_j$ 条)	平均 $D_{\text{par}}$ / $\mu\text{m}$	年龄/Ma
HLK-1	40°56'20"N, 98°31'11"E/1473 m	32	1.173 (4274)	1.6434 (3983)	2.8465 (6899)	29.14	29.5	12.72±1.39 (127)	1.5	118.4±7.3
HLK-2	40°55'17"N, 98°30'28"E/1481 m	32	1.186 (4321)	1.4263 (1765)	2.5536 (3160)	25.68	82.7	12.96±0.25 (105)	1.6	115.9±7.6
HLK-4	40°53'34"N, 98°28'41"E/1517 m	32	1.18 (4297)	2.4206 (3555)	4.4873 (6737)	45.16	50.5	13.01±1.46 (111)	1.57	109±6.8

注： $N_c$ —样品测试的磷灰石颗粒数； $\rho_d$ —用SRM612计量剂计算的白云母外探测器的诱发径迹密度； $N_d$ —诱发径迹总数； $\rho_s$ —自发径迹密度； $N_s$ —自发径迹总数； $\rho_i$ —用晶体分析计算的白云母外探测器的诱发径迹密度； $N_i$ —诱发径迹总数； $P(\chi^2)$ —检验所有单颗粒年龄正态分布置信度的最值(Galbraith, 1981)； $D_{\text{par}}$ —与结晶C轴平行、与抛光面相交的裂变径迹蚀刻象的最大直径； $N_j$ —统计的封闭径迹的条数



a—HLK-1 样品磷灰石裂变径迹年龄雷达图；b—HLK-2 样品磷灰石裂变径迹年龄雷达图；c—HLK-4 样品磷灰石裂变径迹年龄雷达图

$P(\chi^2)$ —检验所有单颗粒年龄正态分布置信度的最值； $D_{\text{par}}$ —与结晶C轴平行、与抛光面相交的裂变径迹蚀刻象的最大直径； $n=32$ —样品测试的磷灰石颗粒数

图7 北山东南部磷灰石裂变径迹年龄的雷达分布图(采用RadialPlotter软件绘制; Vermeesch, 2009)

Fig. 7 Radial plots of apatite fission track ages (plotted from RadialPlotter by Vermeesch, 2009) in the southeastern Beishan Range

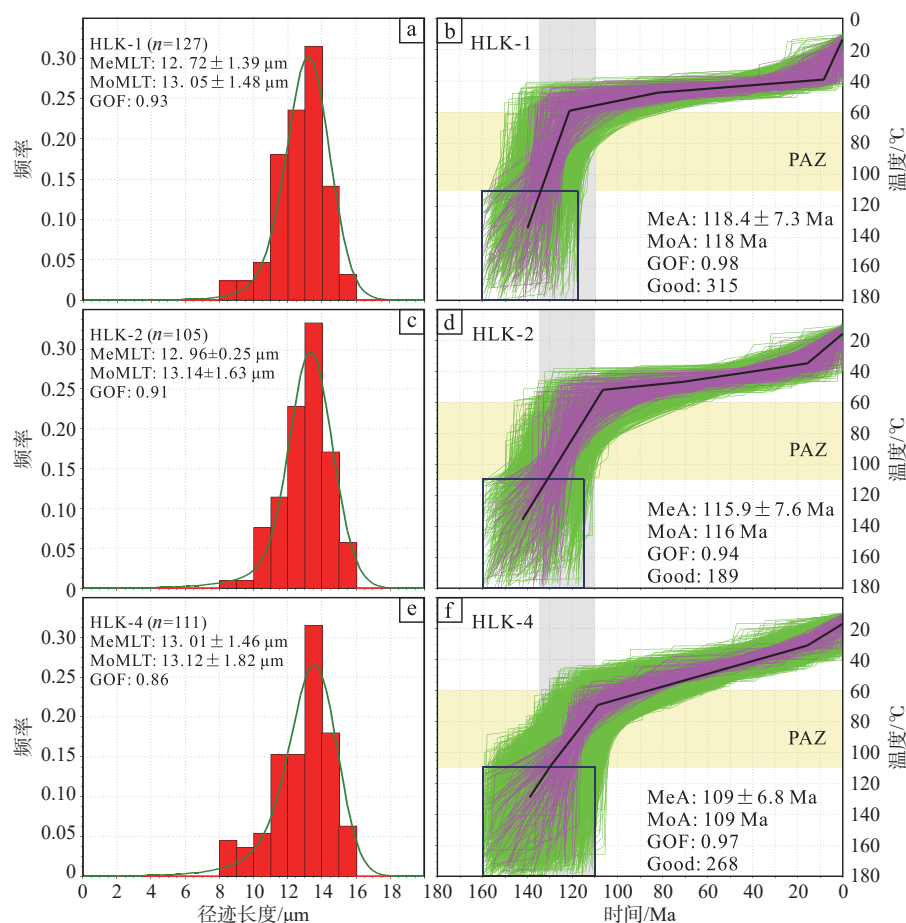
位年龄或地层沉积年龄。因此,这些样品的磷灰石裂变径迹年龄记录了后期构造抬升和剥露过程中的冷却年龄。其中,HLK-1样品的磷灰石裂变径迹年龄较分散( $P(\chi^2)$ (检验所有单颗粒年龄正态分布置信度的最值)为0.295,中值年龄为 $118.4 \pm 7.3$  Ma(图7a);围限平均径迹长度为 $12.72 \pm 1.39 \mu\text{m}$ (图8a),平均 $D_{\text{par}}$ 值为 $1.5 \mu\text{m}$ 。样品HLK-2的磷灰石裂变径迹年龄范围为 $137 \sim 95$  Ma( $P(\chi^2)=0.827$ ),中值年龄为 $115.9 \pm 7.6$  Ma(图7b);围限平均径迹长度为 $12.90 \pm 0.25 \mu\text{m}$ (图8c),平均 $D_{\text{par}}$ 值为 $1.6 \mu\text{m}$ 。样品HLK-4的磷灰石裂变径迹年龄范围为 $131 \sim 96$  Ma( $P(\chi^2)=0.505$ ),中值年龄为 $109 \pm 6.8$  Ma(图7c);围限平均径迹长度为 $13.01 \pm 1.46 \mu\text{m}$ (图8e),平均 $D_{\text{par}}$ 值为 $1.57 \mu\text{m}$ 。由此可见,随着与梭梭井断裂距离的增加,3块样品的磷灰石裂变径迹中值年龄逐渐变小;另外,较长的围限平均径迹长度值( $12.72 \sim 13.01 \mu\text{m}$ )可能反映出样品以较高的冷却速率穿过部分退火带,相似的平均 $D_{\text{par}}$ 值( $1.5 \sim 1.6 \mu\text{m}$ )可能与3块样

品经历了相同的退火行为有关。

### 3.3 热史模拟

利用Hefty软件(v.1.9.1)和Ketcham et al.(2007)多元退火动力学模型及蒙特卡洛逼近法,对磷灰石裂变径迹开展了热史模拟。模拟的基础数据为实测数据,模拟的约束条件:初始温度设定在 $180 \sim 120$  °C,这一温度可使磷灰石裂变径迹完全退火(Green et al., 1989);实测的磷灰石裂变径迹年龄区间,使得样品处于部分退火带( $110 \sim 60$  °C; Ketcham et al., 2007, 2009);现今状态为地表温度( $20 \pm 5$  °C)。每个样品反演模拟10000次,这将允许计算模型统计数据并获得具有代表性的“预期”热史模型。

模拟结果显示,梭梭井断层下盘3块样品经历了相似的冷却过程(图8)。在 $\sim 132$  Ma之前,所有样品均处于完全退火状态(受热温度高于 $120$  °C),随后发生快速冷却。其中,样品HLK-1于 $\sim 132$  Ma冷却至磷灰石裂变径迹封闭温度之下( $\sim 110 \pm 10$  °C)。



PAZ—部分退火带；MeA—实验测试年龄；MoA—模拟年龄；GOF—模拟与实测的拟合度；Good—模拟结果为“好”的热史路径条数；MeMLT—实验测试平均径迹长度；MoMLT—模拟平均径迹长度；——最佳热史路径 ——好的热史路径 ——可接受的热史路径  
 黑色实线代表最佳热史路径，紫色实线代表“好”的热史路径 ( $GOF>0.8$ )，绿色实线代表“可接受”的热史路径 ( $0.8>GOF>0.05$ )  
 a—HLK-1样品磷灰石裂变径迹长度直方分布图；d—HLK-1样品磷灰石裂变径迹热史模拟图；  
 b—HLK-2样品磷灰石裂变径迹长度直方分布图；e—HLK-2样品磷灰石裂变径迹热史模拟图；  
 c—HLK-4样品磷灰石裂变径迹长度直方分布图；f—HLK-4样品磷灰石裂变径迹热史模拟图

图 8 北山东南部磷灰石裂变径迹长度分布图、热史模拟结果及径迹长度实测与模拟结果对比图（热史模拟采用 HeFTy 软件）

Fig. 8 Length distribution of apatite fission tracks, thermal history simulation results, and comparison of measured and simulated track lengths in the southeastern Beishan Range (thermal history simulation results using HeFTy software)

Solid black lines represent the optimal thermal history paths, solid purple lines represent "good" thermal history paths ( $GOF>0.8$ ), and solid green lines represent "acceptable" thermal history paths ( $0.8>GOF>0.05$ ).

℃)，随后快速穿过部分退火带(110~60 ℃)，并于~120 Ma 冷却至部分退火带之下(图 8b)；在 132~120 Ma 期间，样品 HLK-1 的冷却温度至少为~50 ℃，冷却速率超过了~4.1 ℃/Ma。样品 HLK-2 于 132~130 Ma 冷却至磷灰石裂变径迹封闭温度之下，并于~110 Ma 冷却至部分退火带之下(图 8d)；期间样品 HLK-2 的冷却温度为~50 ℃，冷却速率为~2.4 ℃/Ma。样品 HLK-4 于 132~130 Ma 冷却至磷灰石裂变径迹封闭温度之下，并于 132~110 Ma 经历了快速冷却(图 8f)；在~110 Ma 之后，该样品的冷却速率明显变慢，并于~90 Ma 冷却至部分退火带之下；在快速冷却期间(132~110 Ma)，样品 HLK-

4 的冷却温度为~40 ℃，冷却速率为~1.8 ℃/Ma。因此，梭梭井断层下盘于早白垩世晚期(132~110 Ma)经历了快速冷却和剥露事件。

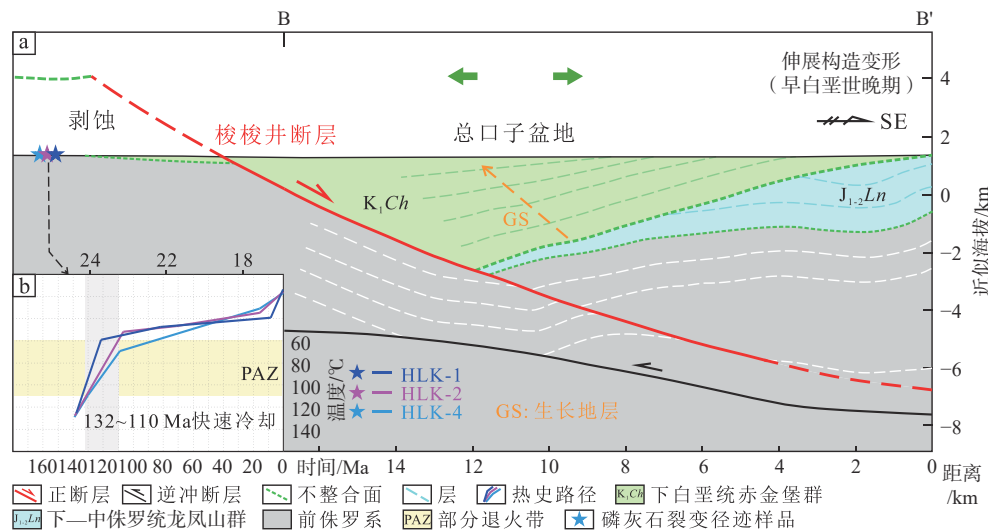
## 4 讨论

### 4.1 伸展变形时间

北山东南部梭梭井断层和五道明断层上盘的下白垩统生长地层发育，其沉积时代为正断层的活动时间。已有研究表明，北山东南部  $K_1Ch$  的沉积时代很可能为早白垩世 Hauterivian-Albian 期(132.6~100 Ma; Li et al., 2007; 张茜楠等, 2015; 张金龙等,

2017; 杨兵等, 2020; 任文秀等, 2022)。磷灰石裂变径迹热史模拟结果显示, 梭梭井断层下盘于132~110 Ma发生了快速冷却和剥露事件。这一快速冷却事件的时间与红旗山逆冲断层下盘的磷灰石(U-Th)/He冷却年龄(124~115 Ma)基本一致, 但小于红旗山逆冲断层上盘的磷灰石(U-Th)/He冷却

年龄(140~133 Ma; 图2a; Liu et al., 2023)。对比分析认为, 梭梭井断层的持续正断层活动控制了132~110 Ma下盘的剥露与快速冷却(图9)。梭梭井断层下盘快速冷却的时间与总口子盆地内K<sub>1</sub>Ch的沉积时代基本一致(图9)。因此, 梭梭井断层和五道明断层的活动时间很可能为早白垩世晚期。



a—北山东南部早白垩世晚期伸展构造模式图; b—磷灰石裂变径迹热史模拟图

图9 北山东南部早白垩世构造-热演化模式图

Fig. 9 The Early Cretaceous tectonic-thermal evolution of the southeastern Beishan Range

(a) Late Early Cretaceous extensional structural deformation pattern in the southeastern Beishan Range; (b) Simulation map of apatite fission track thermal history

区域上, 银额盆地与东戈壁盆地内发育一系列地堑/半地堑盆地(Graham et al., 2001; Johnson et al., 2001; Meng et al., 2003)。这些断陷盆地底部的下白垩统含132~126 Ma安山质玄武岩层(Graham et al., 2001; 陈志鹏等, 2019)。在阿拉善东北缘, 亚干变质核杂岩主拆离断层带内的糜棱岩具129~126 Ma黑云母<sup>40</sup>Ar/<sup>39</sup>Ar冷却年龄, 指示其形成时间(Webb et al., 1999)。此外, 阿拉善至青藏高原东北缘也普遍存在126~100 Ma陆内玄武岩活动(Zhu et al., 2008; Li et al., 2013; Hui et al., 2021), 地球化学特征指示其为陆内伸展与岩石圈减薄的产物(Hui et al., 2021)。上述正断层、断陷盆地、变质核杂岩及玄武岩均形成于早白垩世区域伸展作用过程中。因此, 北山东南部及周缘地区早白垩世伸展构造变形很可能开始于133~129 Ma, 并持续到了早白垩世末期。

#### 4.2 挤压-伸展构造转换及区域意义

中侏罗世晚期—早白垩世早期, 强烈的陆内挤

压变形将古生代—早中生代北山造山带构造活化, 形成了晚中生代北山褶皱-冲断带。期间, 北山逆冲推覆构造发生了大规模(>120 km)由南往北的逆冲运动(左国朝等, 1992; Zheng et al., 1996), 星星峡断层也经历了右行斜向逆冲运动(Zhang and Cunningham, 2012)。在北山东南部, 红柳大泉褶皱-冲断系统沿2个方向同时发生水平缩短, 并吸收了至少~27%的北南向的地壳缩短量, 这使得北山地壳被增厚至50~60 km(Liu et al., 2023)。该期陆内挤压变形事件普遍被认为是亚洲陆缘多板块汇聚作用远程传递的结果, 包括蒙古-鄂霍茨克洋闭合、拉萨与羌塘地体碰撞及古太平洋板块向西俯冲(Zheng et al., 1996; Dumitru and Hendrix, 2001; Guynn et al., 2006; Zhang and Cunningham, 2012; Dong et al., 2015; Van der Voo et al., 2015; Ma et al., 2017; Ma and Xu, 2021)。

早白垩世晚期(133~129 Ma), 区域构造变形

体制发生了重大转变,北山地区及周缘开始转入北西—南东向伸展变形阶段。在北山东南部,梭梭井断层与五道明断层切割了红柳大泉褶皱—冲断系统。其中,梭梭井断层具铲式正断层的特征,往下很可能汇入了一条拆离断层中(脆—韧转换带;图10)。这2条正断层分别限定了早白垩世总口子盆地的北西和南东边界。区域上,阿拉善和南蒙古地区发育一系列同时期的地堑/半地堑盆地(图11;

Graham et al., 2001; Meng, 2003; Wang et al., 2011),其共同组成了早白垩世的伸展盆地系统,如银额盆地(Graham et al., 2001; Meng, 2003; Meng et al., 2003; Hui et al., 2021)。其中,部分断陷盆地具有超拆离盆地的性质,与亚干变质核杂岩及大型拆离断层的形成密切相关(Webb et al., 1999; Meng et al., 2003)。至早白垩世末期,早期增厚的北山地壳(50~60 km)被不同程度地拉伸减薄。

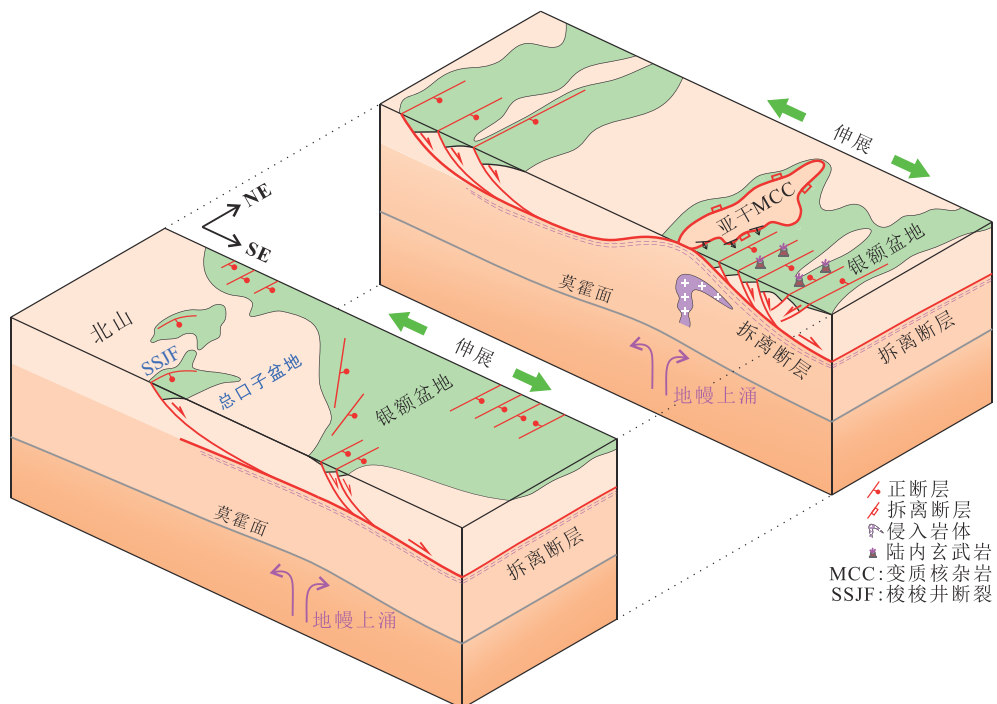


图 10 北山地区及周缘早白垩世伸展构造变形模式图 (Webb et al., 1999; Meng et al., 2003; Hui et al., 2021; Zuo et al., 2020)

Fig. 10 Tectonic model of the Early Cretaceous extensional deformation in the Beishan Range and its surrounding regions (modified from Webb et al., 1999; Meng et al., 2003; Hui et al., 2021; Zuo et al., 2020)

晚中生代中亚造山带南缘普遍经历了挤压—伸展构造的转换(Webb et al., 1999; Johnson et al., 2001; Davis et al., 2002; Cunningham et al., 2009; Wang et al., 2011, 2015; Zhang et al., 2012, 2021a, 2021b; Zhu et al., 2015; Lin and Wei, 2018)。针对这一构造转换,部分学者认为北山、南蒙古和阿拉善地区伸展构造变形开始于晚侏罗世( $\sim 155$  Ma; Zheng et al., 1996; Graham et al., 2001; Johnson et al., 2001; Meng, 2003; Meng et al., 2003)。综合已有成果,研究认为北山地区及周缘晚中生代陆内挤压—伸展构造转换很可能发生在早白垩世晚期(133~129 Ma)。这一构造转换的时间与华北克拉通北缘燕山—阴山构造带及整个东亚地区大规模伸展构造变形的启动时间( $\sim 135$

Ma)基本一致(Davis et al., 2001; 杨进辉等, 2006; Davis and Darby, 2010; 张长厚等, 2011; 刘少峰等, 2018; Wang et al., 2018; Lin et al., 2019, 2020)。同时,伸展构造变形的方向也具有一致性(北西—南东向; Wang et al., 2011; Lin and Wei, 2018; 林伟和李金雁, 2021)。因此,晚中生代中亚造山带南缘很可能经历了统一的陆内挤压—伸展构造转换过程(图11)。

#### 4.3 动力学模式

早白垩世,亚洲陆缘多板块汇聚体系的深部过程和构造体制发生了重大转变(Lin et al., 2013; Dong et al., 2015; Zhu et al., 2015; 张岳桥和董树文, 2019; Ma and Xu, 2021; Chen et al., 2022)。一方面,随着蒙古—鄂霍茨克洋最终关闭,蒙古—鄂霍茨克造山带转

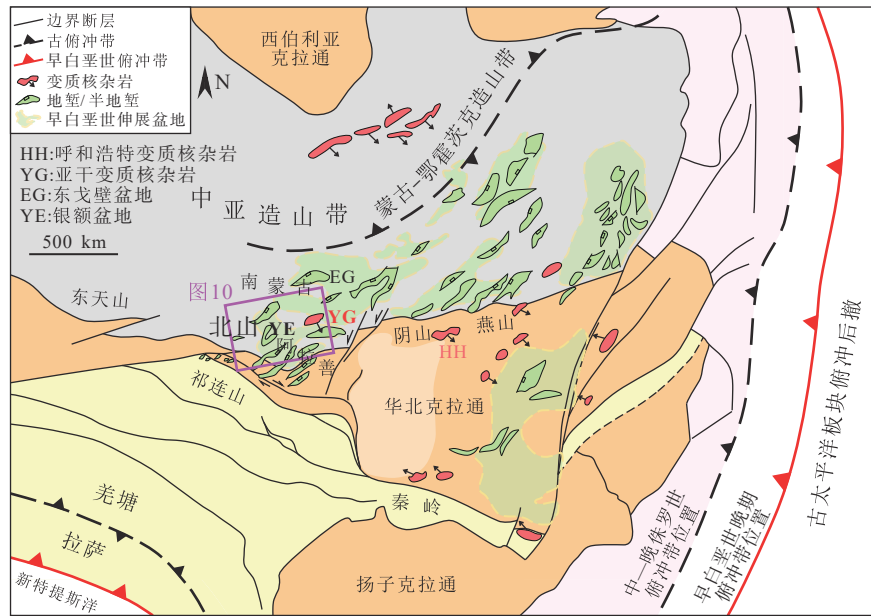


图 11 早白垩世中亚和东亚地区伸展构造变形(包括变质核杂岩和地堑/半地堑盆地等)与亚洲陆缘多板块汇聚体系的关系图 (Meng, 2003; Meng et al., 2003, Wang et al., 2011, 2015; 任纪瞬等, 2013; Lin and Wei, 2018; Ma and Xu, 2021)

Fig. 11 Distribution of Early Cretaceous extensional structures in the central and eastern Asian continent, including metamorphic core complexes and graben/half-graben basins (modified from Meng, 2003; Meng et al., 2003; Wang et al., 2011, 2015; Ren et al., 2013; Lin et al., 2018; Ma and Xu, 2021)

入后造山演化阶段(Meng, 2003; Wang et al., 2011, 2015; 董树文等, 2019)。同时, 拉萨地体与羌塘地体的碰撞拼贴也已基本完成(Fan et al., 2015, 2018; Peng et al., 2020)。因此, 南北向汇聚作用力逐渐减弱(Meng, 2003; 董树文等, 2019; 林伟和李金雁, 2021; Chen et al., 2022)。另一方面, 俯冲的古太平洋板块开始往东回撤, 其俯冲角度也逐渐变陡(图 11; 朱日祥等, 2012; 朱日祥, 2018; 张岳桥和董树文, 2019; Ma and Xu, 2021)。这一重大转变导致区域挤压应力减小甚至消失, 进而引发强烈增厚地壳的重力垮塌。同时, 在中亚造山带南缘曾发现众多早白垩世陆内玄武岩, 表明大量幔源物质加入到了中亚大陆地壳之中, 指示地幔上涌(Graham et al., 2001; Zhu et al., 2008; Li et al., 2013; 陈志鹏等, 2019; Hui et al., 2021)。上涌的地幔物质持续作用于岩石圈底部, 为早白垩世区域伸展作用提供了水平拉伸力(Raimondo et al., 2014; 张进江和黄天立, 2019; Zuo et al., 2020; Hui et al., 2021)。早白垩世古太平洋板块往南东方向发生了大规模俯冲后撤(图 11), 引发了东亚地区软流圈地幔侧向流动或非稳态地幔流(朱日祥等, 2011, 2012; 朱日祥, 2018; Ma and Xu, 2021)。

这一深部地球动力学过程很可能打破了中亚地区地幔对流的原有平衡, 并诱发局部软流圈地幔上涌(Hui et al., 2021; Zuo et al., 2020)。因此, 亚洲陆缘多板块汇聚体系的重大转变诱发了增厚地壳的重力垮塌及局部地幔上涌, 进而导致了中亚造山带南缘早白垩世的区域伸展作用(图 10, 图 11)。

## 5 结论

(1) 在北山东南部, 一系列逆冲断层与褶皱构造造成下—中侏罗统发生强烈挤压变形。二维反射地震剖面揭示出 2 条早白垩世伸展正断层, 其中梭梭井断层为倾向南东的低角度铲式正断层, 五道明断层为倾向北西的高角度正断层。二者均切割了中侏罗世晚期—早白垩世早期的褶皱—冲断系统, 指示挤压—伸展构造的转换。梭梭井断层与五道明断层分别限定了早白垩世总口子盆地的北西和南东边界, 使得其发育“地堑”样式。总口子盆地内下白垩统生长地层发育, 表明梭梭井断层与五道明断层的活动时间为早白垩世晚期。

(2) 磷灰石裂变径迹中值年龄范围为  $118.4 \pm 7.3$

$\text{Ma} \sim 109 \pm 6.8 \text{ Ma}$ 。热史模拟结果显示,梭梭井断层下盘于  $132 \sim 110 \text{ Ma}$  经历了快速冷却和剥露事件,该事件与梭梭井断层的持续正断层活动密切相关。

(3) 北山东南部晚中生代陆内挤-伸展构造转换的时间很可能为  $133 \sim 129 \text{ Ma}$ (早白垩世晚期)。增厚地壳的重力垮塌与局部地幔上涌共同导致了中亚造山带南缘早白垩世北西—南东向伸展构造变形。

**致谢:**感谢中国地震局地质研究所实验测试中心庞建章副研究员提供磷灰石裂变径迹实验测试服务。

## References

- AO S J, XIAO W J, HAN C M, et al, 2012. Cambrian to early Silurian ophiolite and accretionary processes in the Beishan collage, NW China: implications for the architecture of the Southern Altaiids[J]. *Geological Magazine*, 149(4): 606-625.
- Bureau of Geology of Gansu Province (BGGP), Second Regional Geological Survey, 1971. Geologic Map of Hongliudaquan Region, scale 1: 200,000. Beijing, China: Ministry of Geology of China. (in Chinese)
- CHEN B L, DANG G M, CUI W, et al, 2003. Advances in study of crustal stability in Hexi corridor, Northwestern China[J]. *Journal of Geomechanics*, 9(1): 14-20. (in Chinese with English abstract)
- CHEN X H, YIN A, GEHRELS G E, et al, 2003. Two phases of Mesozoic north-south extension in the eastern Altyn Tagh range, northern Tibetan Plateau[J]. *Tectonics*, 22(5): 1053.
- CHEN X H, DANG Y Q, YIN A, et al, 2010. Basin-mountain coupling and tectonic evolution of Qaidam basin and its adjacent orogenic belts[M]. Beijing: Geology Press. (in Chinese)
- CHEN X H, SHAO Z G, XIONG X S, et al, 2019. Fault system, deep structure and tectonic evolution of the Qilian Orogenic Belt, Northwest China[J]. *Geology in China*, 46(5): 995-1020. (in Chinese with English abstract)
- CHEN X H, DONG S W, SHI W, et al, 2022. Construction of the continental Asia in Phanerozoic: A review[J]. *Acta Geologica Sinica-English Edition*, 96(1): 26-51.
- CHEN Z P, REN Z L, QI K, et al, 2019. Zircon U-Pb chronology and geochemistry of volcanic rocks of Early Cretaceous Bayingobi formation in Suhongtu depression of the Ying'e Basin, and their tectonic implications[J]. *Acta Geologica Sinica*, 93(2): 353-367. (in Chinese with English abstract)
- CHENG F, GARZIONE C, JOLIVET M, et al, 2019. Provenance analysis of the Yumen Basin and northern Qilian Shan: Implications for the pre-collisional paleogeography in the NE Tibetan plateau and eastern termination of Altyn Tagh fault[J]. *Gondwana Research*, 65: 156-171.
- CLEVEN N R, LIN S, XIAO W, et al, 2018. Successive arc accretion in the southern Central Asian orogenic belt, NW China: Evidence from two Paleozoic arcs with offset magmatic periods[J]. *Geological Society of America Bulletin*, 130(3-4): 537-557.
- CUNNINGHAM D, 2005. Active intracontinental transpressional mountain building in the Mongolian Altai: Defining a new class of orogen[J]. *Earth and Planetary Science Letters*, 240(2): 436-444.
- CUNNINGHAM D, DAVIES S, MCLEAN D, 2009. Exhumation of a Cretaceous rift complex within a Late Cenozoic restraining bend, southern Mongolia: Implications for the crustal evolution of the Gobi Altai region[J]. *Journal of the Geological Society*, 166(2): 321-333.
- CUNNINGHAM D, 2013. Mountain building processes in intracontinental oblique deformation belts: Lessons from the Gobi Corridor, Central Asia[J]. *Journal of Structural Geology*, 46: 255-282.
- DARBY B J, RITTS B D, 2002. Mesozoic contractional deformation in the middle of the Asian tectonic collage: the intraplate Western Ordos fold-thrust belt, China[J]. *Earth and Planetary Science Letters*, 205(1-2): 13-24.
- DAVIS G A, ZHENG Y D, CONG W, et al, 2001. Mesozoic tectonic evolution of the Yanshan fold and thrust belt, with emphasis on Hebei and Liaoning provinces, northern China[M]//HENDRIX M S, DAVIS G A. Paleozoic and mesozoic tectonic evolution of central and eastern Asia: from continental assembly to intracontinental deformation. Boulder: Geological Society of America Memoir: 171-197.
- DAVIS G A, DARBY B J, ZHENG Y D, et al, 2002. Geometric and temporal evolution of an extensional detachment fault, Hohhot metamorphic core complex, Inner Mongolia, China[J]. *Geology*, 30(11): 1003-1006.
- DAVIS G A, DARBY B J, 2010. Early Cretaceous overprinting of the Mesozoic Daqing Shan fold-and-thrust belt by the Hohhot metamorphic core complex, Inner Mongolia, China[J]. *Geoscience Frontiers*, 1(1): 1-20.
- DONG S W, ZHANG Y Q, ZHANG F Q, et al, 2015. Late Jurassic-Early Cretaceous continental convergence and intracontinental orogenesis in East Asia: A synthesis of the Yanshan Revolution[J]. *Journal of Asian Earth Sciences*, 114: 750-770.
- DONG S W, ZHANG Y Q, LI H L, et al, 2018. The Yanshan orogeny and late Mesozoic multi-plate convergence in East Asia-Commemorating 90th years of the “Yanshan Orogeny” [J]. *Science China Earth Sciences*, 61(12): 1888-1909.
- DUMITRU T A & HENDRIX M. S. 2001. Fission-track constraints on Jurassic folding and thrusting in southern Mongolia and their relationship to the Beishan thrust belt of northern China[J]. *Memoir of the Geological Society of America*, 194, 215-229.
- FAN J J, LI C, XIE C M, et al, 2015. Petrology and U-Pb zircon geochronology of bimodal volcanic rocks from the Maierze Group, northern Tibet: Constraints on the timing of closure of the Banggong-Nujiang Ocean[J]. *Lithos*, 227: 148-160.
- FAN J J, LI C, WANG M, et al, 2018. Reconstructing in space and time the closure of the middle and western segments of the Banggong-Nujiang Tethyan Ocean in the Tibetan Plateau[J]. *International Journal of Earth Sciences*, 107(1): 231-249.
- FENG L M, LIN S F, DAVIS D W, et al, 2018. Dunhuang Tectonic Belt in northwestern China as a part of the Central Asian Orogenic Belt: Structural and U-Pb geochronological evidence[J]. *Tectonophysics*, 747-748: 281-297.
- GALBRAITH R F, 1981. On statistical models for fission track counts[J]. *Journal of the International Association for Mathematical Geology*, 13(6): 471-478.
- GRAHAM S A, HENDRIX M S, JOHNSON C L, et al, 2001. Sedimentary record and tectonic implications of Mesozoic rifting in southeast Mongolia[J]. *GSA Bulletin*, 113(12): 1560-1579.

- GREEN P F, DUDDY I R, LASLETT G M, et al, 1989. Thermal annealing of fission tracks in apatite 4. Quantitative modelling techniques and extension to geological timescales[J]. *Chemical Geology: Isotope Geoscience Section*, 79(2): 155-182.
- GUYNN J H, KAPP P, PULLEN A, et al, 2006. Tibetan basement rocks near Amdo reveal “missing” Mesozoic tectonism along the Bangong suture, central Tibet[J]. *Geology*, 34(6): 505-508.
- HE X Y, FANG T H, BO H T, et al, 2022. Petrogenesis and tectonic significance of Late Permian-Middle Triassic granitoids in Guobaoshan, eastern section of the eastern Tianshan mountains: Constraints from geochronology and geochemistry[J]. *Journal of Geomechanics*, 28(1): 126-142. (in Chinese with English abstract)
- HE Z Y, KLEMD R, YAN L L, et al, 2018. The origin and crustal evolution of microcontinents in the Beishan orogen of the southern Central Asian Orogenic Belt[J]. *Earth-Science Reviews*, 185: 1-14.
- HUI J, CHENG H Y, ZHANG J, et al, 2021. Early Cretaceous continent basalts in the Alxa Block, NW China: geochronology, geochemistry, and tectonic implications[J]. *International Geology Review*, 63(7): 882-899.
- HURFORD A J, GREEN P F, 1983. The zeta age calibration of fission-track dating[J]. *Chemical Geology*, 41: 285-317.
- JIN Y H, CHANG L, JI G, et al, 2020. Chemical characteristics and metallogenetic indications of intrusive rocks in Hongliudaquan area of Beishan[J]. *Mineral Exploration*, 11(1): 10-20. (in Chinese with English abstract)
- JOHNSON C L, WEBB L E, GRAHAM S A, et al, 2001. Sedimentary and structural records of late Mesozoic high-strain extension and strain partitioning, East Gobi basin, southern Mongolia[M]//HENDRIX M S, DAVIS G A. Paleozoic and mesozoic tectonic evolution of central and eastern Asia: from continental assembly to intracontinental deformation. Boulder: Geological Society of America Memoir: 413-433.
- JOLIVET M, BRUNEL M, SEWARD Z X, et al, 2001. Mesozoic and Cenozoic tectonics of the northern edge of the Tibetan plateau: fission-track constraints[J]. *Tectonophysics*, 343(1-2): 0-134.
- JOLIVET M, DOMINGUEZ S, CHARREAU J, et al, 2010. Mesozoic and Cenozoic tectonic history of the Central Chinese Tian Shan: Reactivated tectonic structures and active deformation[J]. *Tectonics*, 29(6): TC6019.
- KETCHAM R A, CARTER A, DONELICK R A, et al, 2007. Improved modeling of fission-track annealing in apatite[J]. *American Mineralogist*, 92(5-6): 799-810.
- KETCHAM R A, DONELICK R A, BALESTRIERI M L, et al, 2009. Reproducibility of apatite fission-track length data and thermal history reconstruction[J]. *Earth and Planetary Science Letters*, 284(3-4): 504-515.
- LI D Q, PENG C, YOU H L, et al, 2007. A large Therizinosauroid (dinosauria: Theropoda) from the Early Cretaceous of northwestern China[J]. *Acta Geologica Sinica-English Edition*, 81(4): 539-549.
- LI J, WU C, CHEN X H, et al, 2023. Tectonic evolution of the Beishan orogen in central Asia: Subduction, accretion, and continent-continent collision during the closure of the Paleo-Asian Ocean[J]. *GSA Bulletin*, 135(3-4): 819-851.
- LI X H, XU W L, LIU W H, et al, 2013. Climatic and environmental indications of carbon and oxygen isotopes from the Lower Cretaceous calcareous and lacustrine carbonates in Southeast and Northwest China[J]. *Palaeogeography, Palaeoclimatology, Palaeoecology*, 385: 171-189.
- LIN C F, LIU S F, SHI X F, et al, 2019. Late Jurassic-Early Cretaceous deformation in the western Yanshan fold - thrust belt: Insights from syntectonic sedimentation in the Chicheng Basin, North China[J]. *Tectonics*, 38(7): 2449-2476.
- LIN W, CHARLES N, CHEN Y, et al, 2013. Late Mesozoic compressional to extensional tectonics in the Yiwulushan massif, NE China and their bearing on the Yinshan-Yanshan orogenic belt: Part II: Anisotropy of magnetic susceptibility and gravity modeling[J]. *Gondwana Research*, 23(1): 78-94.
- LIN W, WEI W, 2018. Late Mesozoic extensional tectonics in the North China Craton and its adjacent regions: a review and synthesis[J]. *International Geology Review*, 62(7-8): 811-839.
- LIN W, LI J Y, 2021. Cretaceous two stage extensional tectonic in eastern Eurasia continent and its geodynamics[J]. *Acta Petrologica Sinica*, 37(8): 2303-2323. (in Chinese with English abstract)
- LIN Y, ZHANG C H, LI C M, et al, 2020. From dextral contraction to sinistral extension of intracontinental transform structures in the Yanshan and northern Taihang Mountain belts during Early Cretaceous: Implications to the destruction of the North China Craton[J]. *Journal of Asian Earth Sciences*, 189: 104139.
- LIU K, CHEN X H, ZUZA A V, et al, 2023. The late Mesozoic intracontinental contraction-extension transition in the Beishan fold-thrust belt, central Asia: Constraints from structural analysis and apatite (U-Th)/He thermochronology[J]. *Tectonics*, 42(7): e2022TC007532.
- LIU S F, LIN C F, LIU X B, et al, 2018. Syn-tectonic sedimentation and its linkage to fold - thrusting in the region of Zhangjiakou, North Hebei, China[J]. *Science China Earth Sciences*, 61(6): 681-710.
- MA A L, HU X M, GARZANTI E D, et al, 2017. Sedimentary and tectonic evolution of the southern Qiangtang basin: Implications for the Lhasa-Qiangtang collision timing[J]. *Journal of Geophysical Research: Solid Earth*, 122(7): 4790-4813.
- MA Q, XU Y G, 2021. Magmatic perspective on subduction of Paleo-Pacific plate and initiation of big mantle wedge in East Asia[J]. *Earth-Science Reviews*, 213: 103473.
- MENG Q R, 2003. What drove late Mesozoic extension of the northern China-Mongolia tract? [J]. *Tectonophysics*, 369(3-4): 155-174.
- MENG Q R, HU J M, JIN J Q, et al, 2003. Tectonics of the late Mesozoic wide extensional basin system in the China-Mongolia border region[J]. *Basin Research*, 15(3): 397-415.
- NIU H Q, HAN X F, WU J, et al, 2021. Age attribution of coal bearing strata in Beishan Basin Group, Ganmeng area[J]. *Bulletin of Geological Science and Technology*, 40(6): 32-42. (in Chinese with English abstract)
- PENG N, LIU Y Q, KUANG H W, et al, 2013. The provenance of Lower Cretaceous basin in the Qilian Mountain-Beishan area: Evidence from paleocurrents, gravels, sandstone compositions and detrital zircon geochronology[J]. *Geological Bulletin of China*, 32(2-3): 456-475. (in Chinese with English abstract)
- PENG Y B, YU S Y, LI S Z, et al, 2020. The odyssey of Tibetan Plateau accretion prior to Cenozoic India-Asia collision: Probing the Mesozoic tectonic evolution of the Bangong-Nujiang Suture[J]. *Earth-Science Reviews*, 211: 103376.
- RAIMONDO T, HAND M, COLLINS W J, 2014. Compressional intracontinental orogens: Ancient and modern perspectives[J]. *Earth-Science Reviews*, 130: 128-153.

- REN J S, NIU B G, WANG J, et al , 2013. International geological map of Asia 1: 5000000[M]. Beijing: Geological Publishing House. (in Chinese)
- REN W X, HU B, TANG D L, et al , 2022. Palynological assemblage and its significance of the Lower Cretaceous Chijinbao Formation in the Zhongkouzi Basin, Beishan area[J/OL]. Earth Science, 1-29. <http://kns.cnki.net/kcms/detail/42.1874.P.20220708.1633.008.html>. (in Chinese with English abstract)
- SONG D F, XIAO W J, HAN C M, et al, 2013. Progressive accretionary tectonics of the Beishan orogenic collage, southern Altaids: Insights from zircon U-Pb and Hf isotopic data of high-grade complexes[J]. *Precambrian Research*, 227: 368-388.
- TANG W D, HE J L, LIU T H, et al, 2023. Geochemical characteristics of the garnets from the Laodonggou gold deposit, Beishan, Inner Mongolia[J]. *Journal of Geomechanics*, 29(1): 60-75. (in Chinese with English abstract)
- VAN DER VOO R, VAN HINSBERGEN D J J, DOMEIER M, et al , 2015. Latest Jurassic-earliest Cretaceous closure of the Mongol-Okhotsk Ocean: A paleomagnetic and seismological-tomographic analysis[M]//ANDERSON T H, DIDENKO A N, JOHNSON C L, et al Late Jurassic margin of Laurasia-a record of faulting accommodating plate rotation. Boulder: The Geological Society of America: 589-606.
- VERMEESCH P, 2009. RadialPlotter: a Java application for fission track, luminescence and other radial plots[J]. *Radiation Measurements*, 44(4): 409-410.
- WANG T, ZHENG Y D, ZHANG J J, et al, 2011. Pattern and kinematic polarity of late Mesozoic extension in continental NE Asia: Perspectives from metamorphic core complexes[J]. *Tectonics*, 30(6): TC6007.
- WANG T, GUO L, ZHANG L, et al, 2015. Timing and evolution of Jurassic-Cretaceous granitoid magmatisms in the Mongol-Okhotsk belt and adjacent areas, NE Asia: Implications for transition from contractional crustal thickening to extensional thinning and geodynamic settings[J]. *Journal of Asian Earth Sciences*, 97: 365-392.
- WANG Y, SUN G H, LI J Y, 2010. U-Pb (SHRIMP) and  $^{40}\text{Ar}/^{39}\text{Ar}$  geological constraints on the evolution of the Xingxingxia shear zone, NW China: A Triassic segment of the Altyn Tagh fault system[J]. *GSA Bulletin*, 122(3-4): 487-505.
- WANG Y, CHEN X H, ZHANG Y Y, et al, 2022. Superposition of Cretaceous and Cenozoic deformation in northern Tibet: A far-field response to the tectonic evolution of the Tethyan orogenic system[J]. *GSA Bulletin*, 134(1-2): 501-525.
- WANG Y C, DONG S W, CHEN X H, et al, 2018. Yanshanian deformation along the northern margin of the North China Craton: Constraints from growth strata in the Shiguai Basin, Inner Mongolia, China[J]. *Basin Research*, 30(6): 1155-1179.
- WEBB L E, GRAHAM S A, JOHNSON C L, et al, 1999. Occurrence, age, and implications of the Yagan-Onch Hayrhan metamorphic core complex, southern Mongolia[J]. *Geology*, 27(2): 143-146.
- XIAO W J, MAO Q G, WINDLEY B F, et al, 2010. Paleozoic multiple accretionary and collisional processes of the Beishan orogenic collage[J]. *American Journal of Science*, 310(10): 1553-1594.
- XU X Y, LI R S, WANG H L, et al , 2015. Geological map of northwest China, scale 1: 1000 000. Xi'an, China, Xi'an Center, China Geological Survey.
- YANG B, LI S C, WEI N Y, et al, 2020. The discovery of ostracods assemblages from Early Cretaceous Chijinpu formation in Tianchang area, Ji-quan, Gansu province, and its geological significance[J]. *Geological Bulletin of China*, 39(4): 433-441. (in Chinese with English abstract)
- YANG J H, WU F Y, SHAO J A, et al, 2006. In-Situ U-Pb Dating and Hf isotopic analyses of zircons from volcanic rocks of the Houcheng and Zhangjiakou formations in the Zhang-Xuan area, northeast China[J]. *Earth Science*, 31(1): 71-80. (in Chinese with English abstract)
- YIN A, NIE S, CRAIG P, et al, 1998. Late Cenozoic tectonic evolution of the southern Chinese Tian Shan[J]. *Tectonics*, 17(1): 1-27.
- YUN L, ZHANG J, WANG J, et al, 2021. Discovery of active faults in the southern Beishan area, NW China: Implications for regional tectonics[J]. *Journal of Geomechanics*, 27(2): 195-207. (in Chinese with English abstract)
- ZHANG B L, ZHU G, JIANG D Z, et al, 2012. Evolution of the Yiwulushan metamorphic core complex from distributed to localized deformation and its tectonic implications[J]. *Tectonics*, 31(4): TC4018.
- ZHANG C H, LI C M, DENG H L, et al, 2011. Mesozoic contraction deformation in the Yanshan and northern Taihang mountains and its implications to the destruction of the North China Craton[J]. *Science China Earth Sciences*, 54(6): 798-822.
- ZHANG J, CUNNINGHAM D, 2012. Kilometer-scale refolded folds caused by strike-slip reversal and intraplate shortening in the Beishan region, China[J]. *Tectonics*, 31(3): TC3009.
- ZHANG J, WANG Y N, QU J F, et al, 2021a. Mesozoic intracontinental deformation of the Alxa Block in the middle part of Central Asian Orogenic Belt: A review[J]. *International Geology Review*, 63(12): 1490-1520.
- ZHANG J, WANG Y N, ZHANG B H, et al, 2021b. Tectonothermal events in the central North China Craton since the Mesozoic and their tectonic implications: Constraints from low-temperature thermochronology[J]. *Tectonophysics*, 804: 228769.
- ZHANG J, CUNNINGHAM D, QU J F, et al, 2022. Poly-phase structural evolution of the northeastern Alxa Block, China: Constraining the Paleozoic-Recent history of the southern central Asian Orogenic belt[J]. *Gondwana Research*, 105: 25-50.
- ZHANG J J, HUANG T L, 2019. An overview on continental extensional tectonics[J]. *Earth Science*, 44(5): 1705-1715. (in Chinese with English abstract)
- ZHANG J L, CHEN C, ZHANG G F, et al , 2017. Sedimentary characteristics and age of the Early Cretaceous Chijinbao formation in the Sandaoingshui of Beishan area, Inner Mongolia[J]. *Geological Survey and Research*, 40(1): 29-34, 80. (in Chinese with English abstract)
- ZHANG Q N, YOU H L, LI D Q, 2015. Dinosaurs from late early cretaceous in the Mazongshan area, Gansu province[J]. *Geological Bulletin of China*, 34(5): 890-897. (in Chinese with English abstract)
- ZHANG Y, DONG S W, SHI W, 2024. Hohhot thermal upwelling-extensional structure: Recognition of “metamorphic core complexes” in North China[J]. *Chinese Science Bulletin*, 68(7): 939-949. (in Chinese with English abstract)
- ZHANG Y Q, DONG S W, 2019. East Asia multi-plate convergence in Late Mesozoic and the development of continental tectonic systems[J]. *Journal of Geomechanics*, 25(5): 613-641. (in Chinese with English abstract)
- ZHENG Y, ZHANG Q, WANG Y, et al, 1996. Great Jurassic thrust sheets in Beishan (North Mountains)-Gobi areas of China and southern Mongolia[J]. *Journal of Structural Geology*, 18(9): 1111-1126.
- ZHU G, CHEN Y, JIANG D Z, et al, 2015. Rapid change from compression

- to extension in the North China Craton during the Early Cretaceous: Evidence from the Yunmengshan metamorphic core complex[J]. *Tectonophysics*, 656: 91-110.
- ZHU R X, PAN Y X, HE H Y, et al, 2008. Palaeomagnetism and  $^{40}\text{Ar}/^{39}\text{Ar}$  age from a Cretaceous volcanic sequence, Inner Mongolia, China: Implications for the field variation during the Cretaceous normal superchron[J]. *Physics of the Earth and Planetary Interiors*, 169(1-4): 59-75.
- ZHU R X, CHEN L, WU F Y, et al, 2011. Timing, scale and mechanism of the destruction of the North China Craton[J]. *Science China Earth Sciences*, 54(6): 789-797.
- ZHU R X, XU Y G, ZHU G, et al, 2012. Destruction of the North China Craton[J]. *Science China Earth Sciences*, 55(10): 1565-1587.
- ZHU R X, 2018. Review of the achievement of major research plan on “Destruction of North China Craton” [J]. *Bulletin of National Natural Science Foundation of China*, 32(3): 282-290. (in Chinese with English abstract)
- ZUO G C, ZHANG S L, HE G Q, et al, 1991. Plate tectonic characteristics during the early Paleozoic in Beishan near the Sino-Mongolian border region, China[J]. *Tectonophysics*, 188(3-4): 385-392.
- ZUO G C, FENG Y Z, LIU C Y, et al, 1992. A new discovery of early Yan Shanian strike-slip compressional nappe zones on middle-southern segment of Beishan mts, Gansu[J]. *Chinese Journal of Geology*(4): 309-316. (in Chinese with English abstract)
- ZUO Y H, JIANG S, WU S H, et al, 2020. Terrestrial heat flow and lithospheric thermal structure in the Chagan depression of the Yingen-Ejin- aqi basin, North Central China[J]. *Basin Research*, 32(6): 1328-1346.
- ZUZA A V, WU C, REITH R C, et al, 2018. Tectonic evolution of the Qilian Shan: An early Paleozoic orogen reactivated in the Cenozoic[J]. *GSA Bulletin*, 130(5-6): 881-925.
- 靳拥护, 常磊, 姬果, 等, 2020. 北山红柳大泉地区侵入岩岩石化学特征及成矿指示意义[J]. *矿产勘查*, 11(1): 10-20.
- 林伟, 李金雁, 2021. 欧亚大陆东部白垩纪两期伸展穹隆构造及其动力学机制探讨[J]. *岩石学报*, 37(8): 2303-2323.
- 刘少峰, 林成发, 刘晓波, 等, 2018. 冀北张家口地区同构造沉积过程及其与褶皱-逆冲作用耦合[J]. *中国科学: 地球科学*, 48(6): 705-731.
- 牛海青, 韩小锋, 吴俊, 等, 2021. 甘蒙地区北山盆地群含煤系地层时代归属[J]. *地质科技通报*, 40(6): 32-42.
- 彭楠, 柳永清, 旷红伟, 等, 2013. 北祁连—北山地区早白垩世盆地物源分析: 来自古水流、砾石组分、砂岩组分和碎屑锆石年龄的证据[J]. *地质通报*, 32(2-3): 456-475.
- 任纪舜, 牛宝贵, 王军, 等, 2013. 国际亚洲地质图(1: 5000000) [M]. 北京: 地质出版社.
- 任文秀, 胡斌, 唐德亮, 等, 2022. 北山地区中口子盆地下白垩统赤金堡组孢粉组合及其意义 [J/OL]. *地球科学*, 1-29. <http://kns.cnki.net/kcms/detail/42.1874.P.20220708.1633.008.html>.
- 唐卫东, 何佳乐, 刘天航, 等, 2023. 内蒙古北山老硐沟金矿石榴子石地球化学特征[J]. *地质力学学报*, 29(1): 60-75.
- 徐学义, 李荣社, 王洪亮, 等, 2015. 中国西北地区地质图(1: 100万). 中国地质调查局西安地质调查中心.
- 杨兵, 李树才, 魏乃顾, 等, 2020. 甘肃酒泉市天仓地区早白垩世介形类的发现及其地质意义[J]. *地质通报*, 39(4): 433-441.
- 杨进辉, 吴福元, 邵济安, 等, 2006. 冀北张-宣地区后城组、张家口组火山岩锆石 U-Pb 年龄和 Hf 同位素[J]. *地球科学*, 31(1): 71-80.
- 云龙, 张进, 王驹, 等, 2021. 甘肃北山南部活动断裂的发现及其区域构造意义[J]. *地质力学学报*, 27(2): 195-207.
- 张长厚, 李程明, 邓洪菱, 等, 2011. 燕山-太行山北段中生代收缩变形与华北克拉通破坏[J]. *中国科学: 地球科学*, 41(5): 593-617.
- 张进江, 黄天立, 2019. 大陆伸展构造综述[J]. *地球科学*, 44(5): 1705-1715.
- 张金龙, 陈超, 张桂凤, 等, 2017. 内蒙古北山地区三道明水一带早白垩世赤金堡组沉积特征及时代厘定[J]. *地质调查与研究*, 40(1): 29-34, 80.
- 张茜楠, 尤海鲁, 李大庆, 2015. 甘肃马鬃山地区早白垩世晚期恐龙化石[J]. *地质通报*, 34(5): 890-897.
- 张宇, 董树文, 施炜, 2024. 呼和浩特热隆伸展构造: 华北“变质核杂岩”再认识[J]. *科学通报*, 68(7): 939-949.
- 张岳桥, 董树文, 2019. 晚中生代东亚多板块汇聚与大陆构造体系的发展[J]. *地质力学学报*, 25(5): 613-641.
- 朱日祥, 陈凌, 吴福元, 等, 2011. 华北克拉通破坏的时间、范围与机制[J]. *中国科学: 地球科学*, 41(5): 583-592.
- 朱日祥, 徐义刚, 朱光, 等, 2012. 华北克拉通破坏[J]. *中国科学: 地球科学*, 42(8): 1135-1159.
- 朱日祥, 2018. “华北克拉通破坏”重大研究计划结题综述[J]. *中国科学基金*, 32(3): 282-290.
- 左国朝, 冯永忠, 刘春燕, 等, 1992. 甘蒙北山中南带新发现燕山早期走滑挤压推覆构造带[J]. *地质科学*(4): 309-316.

## 附中文参考文献

- 陈柏林, 党光明, 崔巍, 等, 2003. 河西走廊地壳稳定性研究进展[J]. *地质力学学报*, 9(1): 14-20.
- 陈宣华, 党玉琪, 尹安, 等, 2010. 柴达木盆地及其周缘山系盆地耦合与构造演化[M]. 北京: 地质出版社.
- 陈宣华, 邵兆刚, 熊小松, 等, 2019. 祁连造山带断裂构造体系、深部结构与构造演化[J]. *中国地质*, 46(5): 995-1020.
- 陈志鹏, 任战利, 祁凯, 等, 2019. 银额盆地苏红图坳陷早白垩世巴音戈壁组火山岩锆石 U-Pb 年代学、地球化学特征及构造意义[J]. *地质学报*, 93(2): 353-367.
- 董树文, 张岳桥, 李海龙, 等, 2019. “燕山运动”与东亚大陆晚中生代多板块汇聚构造: 纪念“燕山运动”90周年[J]. *中国科学: 地球科学*, 49(6): 913-938.
- 甘肃省地质局, 第二区域地质调查队, 1971. 1: 20 万红柳大泉幅. 中国地质矿产局.
- 贺昕宇, 方同辉, 薄贺天, 等, 2022. 东天山东段国宝山晚二叠世—中三叠世花岗质岩石成因与构造意义: 年代学和地球化学约束[J]. *地质力学学报*, 28(1): 126-142.